Results in Physics 67 (2024) 108050

Contents lists available at ScienceDirect

Results in Physics

journal homepage: www.elsevier.com/locate/rinp

Asymptotic normalization coefficients for $^{11}B + p \rightarrow {}^{12}C$ from the $^{11}B(^{10}B, {}^{9}Be)^{12}C$ reaction and the $^{11}B(p, \gamma)^{12}C$ astrophysical *S*-factor

S.K. Sakhiyev [a], S.V. Artemov [a,b], N. Burtebayev [a,c], S.B. Sakuta [a,d], S.B. Igamov [b,e], Maulen Nassurlla [a,c], K. Rusek [f], M. Wolińska-Cichocka [f], N. Amangeldi [a,g], Marzhan Nassurlla [a], A. Trzcińska [f], G. Yergaliuly [a,g], F.Kh. Ergashev [b], O.R. Tojiboev [b], I.Ya. Son [b,*], A. Sabidolda [a], R. Khojayev [a,c], Y.B. Mukanov [a,c], D.A. Issayev [a,c]

[a] Institute of Nuclear Physics, 050032 Almaty, Kazakhstan
[b] Institute of Nuclear Physics, 100214 Tashkent, Uzbekistan
[c] Al-Farabi Kazakh National University, 050040 Almaty, Kazakhstan
[d] National Research Center "Kurchatov Institute", 123182 Moscow, Russia
[e] Branch of National Research Nuclear University MEPhI, 100214 Tashkent, Uzbekistan
[f] Heavy Ion Laboratory, University of Warsaw, PL-02-093 Warsaw, Poland
[g] L.N. Gumilyov Eurasian National University, 010008 Astana, Kazakhstan

ARTICLE INFO

Keywords:
Heavy ion beam
peripheral proton transfer
modified distorted wave Born approximation (MDWBA)
asymptotic normalization coefficient (ANC)
astrophysical *S*-factor

ABSTRACT

The $^{11}B(^{10}B,^{9}Be)^{12}C$ reaction was studied at the energy of 41.3 MeV with transitions to the ground (0^+) and low-lying excited 4.44 MeV (2^+) and 9.64 MeV (3^-) states of ^{12}C nucleus. The analysis of the measured angular distributions was carried out using a modified distorted wave (MDWBA) method, assuming a one-step proton transfer mechanism. It was shown that at small angles (in the region of the main diffraction maximum) this reaction occurs on the nuclear surface with the dominance of a one-step process. This made possible to determine the values of asymptotic normalization coefficients (ANC) for $^{11}B + p \rightarrow {}^{12}C$. The squared ANCs equal to 322 ± 76 fm^{-1}, 32.8 ± 8.4 fm^{-1} and 1.26 ± 0.44 fm^{-1} for 0^+, 2^+ and 3^- states of the ^{12}C nucleus respectively were obtained. These values were used to take into account the contribution of the direct process in the calculation of astrophysical *S*-factors for the radiative capture of a proton by the ^{11}B nucleus at astrophysical energies.

Introduction

To substantiate theoretical models of stellar evolution it is extremely important to understand the formation pathways of CNO nuclei. It is generally accepted that ^{12}C nuclei are formed in the Universe mainly due to the fusion of three α particles through a second 0^+ state, located at excitation energy of 7.65 MeV, which is 0.38 MeV above the 3α threshold and called the Hoyle state [1]. This is due to the fact that the temperature and density of ^{4}He nuclei in the cores of red giant stars is quite high.

However, other possibilities for bridging the gap at mass number A = 8 are also being considered. In Refs. [2–4] the production of CNO material bypassing 3α mechanism in inhomogeneous big bang nucleosynthesis (IBBN) scenarios was discussed.

In this case, the main chain of ^{12}C nucleus formation in several models (with the ratio of the baryon density to the critical energy density, $\Omega_b = 1$) is the sequence of reactions:

$^{1}H(n, \gamma)^{2}H(n, \gamma)^{3}H(^{2}H, n)^{4}He(^{3}H, \gamma)^{7}Li(n, \gamma)^{8}Li(^{4}He, n)^{11}B(n, \gamma)^{12}B(\beta-)^{12}C(n, \gamma)\ldots$

Authors of Ref. [5] noted that at lower values of Ω_b, the reaction $^{7}Li(\alpha,\gamma)^{11}B$ is an alternative for this chain. Their assessments [5] showed that the reaction $^{11}B(d,n)^{12}C$ may well compete with the subsequent processes $^{11}B(n,\gamma)^{12}B(\beta^{-}\nu)^{12}C$. In this regard, the astrophysical *S*-factors of this reaction were measured in Ref. [4] at astrophysically relevant energies of 120–160 keV.

Direct proton capture by the ^{11}B nucleus is often neglected due to the large Coulomb barrier and small cross section at astrophysically relevant energies. However, proton capture by ^{11}B cannot be neglected in the BBN scenarios as well as in stellar nucleosynthesis. He et al. [6] determined the astrophysical *S*-factors of the $^{11}B(p,\gamma)^{12}C$ reaction for capture

* Corresponding author.
E-mail address: son.irina@inp.uz (I.Ya. Son).

https://doi.org/10.1016/j.rinp.2024.108050
Received 2 August 2024; Received in revised form 6 October 2024; Accepted 16 November 2024
Available online 20 November 2024

on the ground and the first excited state of ^{12}C in the energy range $E_{c.m.}$ = 130–257 keV, where the possible significance of the ^{11}B(p,γ)^{12}C process at low energies is emphasized. As noted in Ref. [2] in the processes of nucleosynthesis in proton-rich environment typical for supermassive stars with low metallicity at very high temperatures and densities, the hot *pp* chain can bypass the slower 3α capture. Among the chains of nuclear reactions that become important in this case is the chain:

…^{7}Be(α,γ){or ^{7}Be(p,γ)^{8}B(α,p)}^{11}C(e$^{+}\nu$)^{11}B(p,γ)^{12}C.

Thus, reactions (p,γ) and (d,n) are of certain interest when analyzing scenarios for the nucleosynthesis of CNO nuclei.

It should be noted that direct measurements of the total cross sections of the radiative proton capture by ^{11}B nuclei, even at not too low energies, is non-trivial experimental task, since one should measure low-intensity γ-spectra with energies $E_\gamma > 10$ MeV [6].

At the same time, to extrapolate the *S*-factors of both of these reactions to the astrophysical relevant energies ($E_p < 100$ keV), it is necessary to know the correct values of the asymptotic normalization coefficients (ANC) for bound proton states in the ^{12}C nucleus in addition to the characteristics of existing resonances Refs. [7,8]. In the energy region below 100 keV, there are no resonances in the ^{11}B + p system; therefore, the contribution of the direct and interference parts to the reaction amplitude, determined by the ANC value, becomes significant. To date, directly from the analysis of experimental data, only in Ref. [9] the ANC values for proton binding in several states of the ^{12}C nucleus populated in the reaction (^{3}He, d) have been obtained. These data are not entirely reliable, since the transitions of the proton to the lower strongly bound states turned out to be non-peripheral, and the range of uncertainty in the found values of the ANC is large. Moreover, their central values may be shifted because they are extracted under the assumption that the geometric parameters of the Woods-Saxon (WS) binding potential of a proton in the ^{12}C nucleus have "standard" values (r_0 = 1.25 fm and a = 0.65 fm).

As noted in Ref. [8], reactions of the A(^{10}B, ^{9}Be)B type are a fairly convenient tool for defining the characteristics of single-particle (proton) states B = A + p, since the proton binding energy of the ^{10}B nucleus is rather small (ε_p = 6.586 MeV), and the ^{9}Be nucleus does not have nuclear-stable excited states. In addition, the value of the ANC of the overlap integral ^{10}B$_{g.s.}$={^{9}Be + p} has been studied in a number of works and is quite well known.

The purpose of this work is to determine the ANC values for low-lying bound proton states in the ^{12}C nucleus from a thorough analysis of the obtained experimental data on the ^{11}B(^{10}B,^{9}Be)^{12}C reaction. This requires a careful evaluation of the peripherality of proton transfer in the region of the main maximum of the angular distribution of differential cross sections (DCSs), as well as taking into account the contribution of reaction mechanisms other than one-step proton transfer. The extracted ANC values for the ground (0^+) and excited (2^+) states of the ^{12}C nucleus, for which radiative capture makes a dominant contribution to the total *S*-factor of the ^{11}B(p, γ)^{12}C reaction, are then used in calculating the *S*-factor within the modified *R*-matrix approach [10–13].

Experimental procedure and measurement results

The angular distributions of ^{9}Be from the ^{11}B(^{10}B,^{9}Be)^{12}C reaction were measured with a ^{10}B beam extracted from the U-200P cyclotron of the Heavy-Ion Laboratory of the University of Warsaw. The measurement technique is described in sufficient detail in our other works using a beam of ^{10}B ions [8,14], so here we present only the main details of the experiment.

The energy of the ^{10}B ions was 41.3 MeV with a spread of no more than 1 %. The beam was directed to the boron target in the scattering chamber of the multi-detector ICARE setup which is shown in Fig. 1 in Ref. [15]. The products of nuclear reactions were detected by four $\Delta E - E$ telescopes consisting of silicon detectors (E) about 500 μm thick and ionization chambers (ΔE) filled with isobutane (C_4H_{10}) to a pressure of

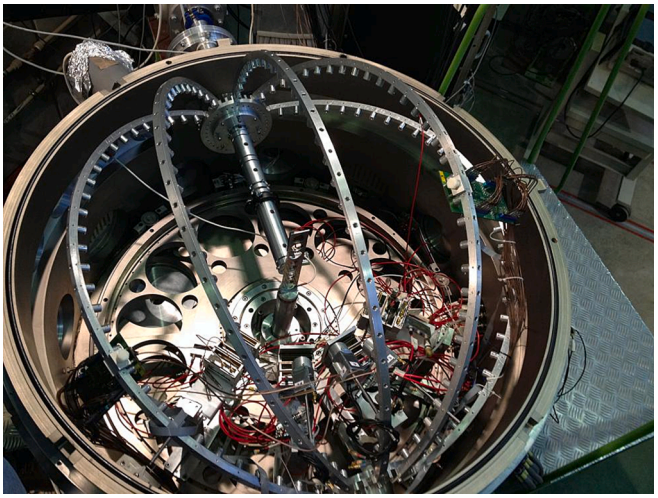

Fig. 1. Scattering chamber of the multi-detector ICARE setup.

∼ 55 Torr. The telescopes were mounted in pairs on two remotely rotating platforms.

Each ionization chamber has the shape of a truncated cone 50 mm long with an entrance window made of Mylar 2.5 μm thick. Detector E is placed at the end of the ionization chamber directly in the gas volume. Also, three monitor silicon detectors were installed outside the telescope rotation plane at angles of 15° to measure and control the beam energy, as well as the target state. The charge of the beam passing through the target was collected in a Faraday cup and integrated with an accuracy of no worse than 1 %. Thickness of boron targets enriched with the ^{11}B isotope to 96 % was about 0.14 mg/cm^2, which was measured by the loss of energy of alpha particles from a radioactive source. For its manufacture, the vacuum evaporation installation of the Institute of Nuclear Physics of the Republic of Kazakhstan was applied [16].

Standard CAMAC electronics and the MIDAS and SMAN data acquisition systems [17] were used. The data obtained were processed by the ROOT program [18]. A typical two-dimensional ($\Delta E, E$) spectrum is shown in Fig. 2.

One can see a good separation of the reaction products with charges of Z = 2–7, which is enough to obtain the required DCS. For the lightest reaction products (lithium and beryllium), separation by mass is also achieved (^{6}Li and ^{7}Li; ^{7}Be and ^{9}Be), and the corresponding loci are bifurcated. An example of energy spectrum of ^{9}Be nuclei arising from the ^{11}B+^{10}B interaction is shown in Fig. 3.

The overall energy resolution in the spectrum is about 500 keV, which is determined mainly by the statistically independent contribution from the target thickness (∼300 keV), the resolution of the telescope *E*-detectors (∼300–350 keV) and the energy spread of accelerated 10B ions (∼200 keV).

The angular distributions of ^{9}Be from the ^{11}B(^{10}B,^{9}Be)^{12}C reaction were measured for three transitions to low-lying states of the ^{12}C nucleus in the angular range 5°–43°in the laboratory system. They are shown in Fig. 6. All measured angular distributions are characterized by a weakly expressed diffraction structure. The statistical errors are 2–13 % (more exactly, 3–13 % for ground state, 2–10 % for the 1st excited state and 2–12 % for the 3rd excited state of the ^{12}C nucleus, respectively). According to our estimates, the systematic errors of the DCS values are determined mainly by errors in measuring the thickness of the target (6–8 %), determining the solid angles of telescopes (5 %) estimating errors in the recording system due to pulse overlap (2–3 % at small measurement angles), and integration of the beam current (1%), which amounts to 10% in total. An additional check in determining the absolute value of the experimental DCS was performed by comparing the cross section of the elastic scattering of the ^{10}B ions on ^{11}B nuclei at small angles with the cross section for Rutherford scattering. Overall, we

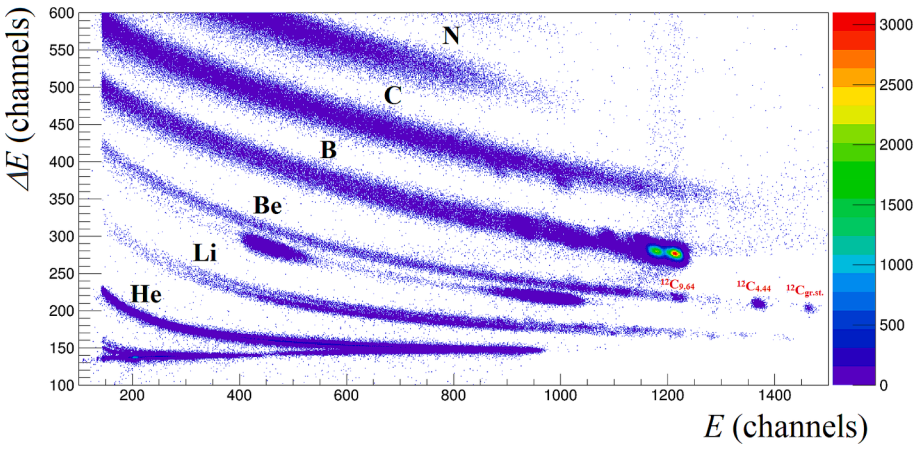

Fig. 2. Two-dimensional $(\Delta E, E)$ spectrum of charged particles from the interaction of ^{10}B with a target, measured at $\theta_{\text{lab}} = 12^{\circ}$.

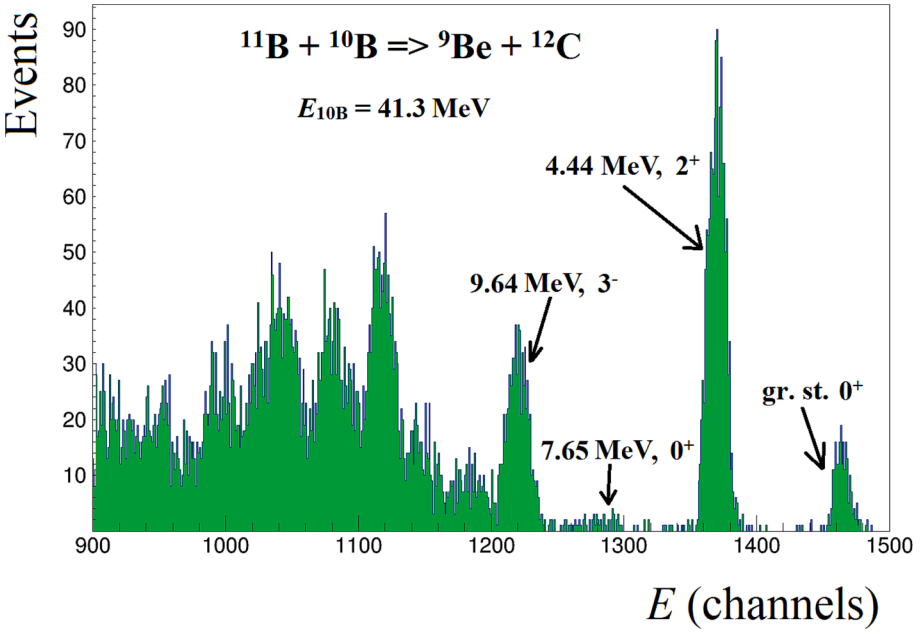

Fig. 3. Fragment of the ^{9}Be energy spectrum from the ^{11}B(^{10}B,^{9}Be)^{12}C reaction at $E_{\text{lab}}(^{10}\text{B}) = 41.3$ MeV measured at $\theta_{\text{lab}} = 12^{\circ}$. The arrows indicate the positions of peaks corresponding to the low-lying states of the ^{12}C nucleus.

estimated the absolute errors of the measured DCS at no more than 11% in the region of the main maximum of the angular distribution.

Analysis of the proton transfer reaction and the asymptotic normalization coefficient FOR $^{11}\text{B} + p \rightarrow {}^{12}\text{C}$

MDWBA analysis

Here we present the results of the analysis of experimental DCS for the ^{11}B(^{10}B, ^{9}Be)^{12}C proton transfer reaction, measured by us at a projectile energy of 41.3 MeV with transitions to the ground (0^{+}), as well as to excited, E^{*}= 4.44 MeV (2^{+}) and 9.64 MeV (3^{-}) states of the ^{12}C nucleus. The experimental DCSs for the state $E^{*} = 7.65$ MeV (0^{+}) were not extracted from our data because of very poor statistics. The poor statistics is explained by the fact that this Hoyle state does not have a single-particle structure, that in turn leads to a strong decrease in the cross section for the ^{11}B(^{10}B, ^{9}Be)^{12}C proton transfer reaction. The method combining DWBA and the dispersion approach to the analysis of direct nuclear reactions, the basis of which was proposed in Refs. [19,20] and then developed in subsequent works (see the review article [21] and references therein), is currently widely used to extract ANCs from data on peripheral nuclear reactions. DCS ($\frac{d\sigma}{d\Omega}^{\text{MDW}}$) within the framework of the MDWBA for the peripheral reaction of proton stripping A(x,y)B, where $x = y + p$ and B $=$ A $+ p$, at fixed relative energy E in the channel A $+x$ and the outgoing angle θ of particle y, as well as assuming that only one value of the orbital momentum ℓ of the transferred proton in nucleus B dominates, has the form [8,22,23]:

$$\frac{d\sigma}{d\Omega}^{\text{MDW}}(E,\theta;b_{x\to y+p},b_{\text{B}\to\text{A}+p;\ell j}) = C^{2}_{\text{B}\to\text{A}+p;\ell j+}\left[R_{j+}\left(E,\theta;b_{x\to y+p},b_{\text{B}\to\text{A}+p;\ell j+}\right)+\lambda R_{j-}\left(E,\theta;b_{x\to y+p},b_{\text{B}\to\text{A}+p;\ell j-}\right)\right] \quad (1)$$

$$R(E,\theta;b_{x\to y+p},b_{\mathrm{B}\to\mathrm{A}+p})=\frac{C^2_{x\to y+p}}{b^2_{x\to y+p}}\,\frac{\sigma^{\mathrm{DW}}(E,\theta;b_{x\to y+p},b_{\mathrm{B}\to\mathrm{A}+p;\ell j})}{b^2_{\mathrm{B}\to\mathrm{A}+p;\ell j}} \quad (2)$$

Here, $C_{\mathrm{B}\to\mathrm{A}+p}$ and $C_{x\to y+p}$ are the ANCs for the A$+p\to$B and $y+p\to x$ systems, which determine the amplitudes of the tails of the radial wave functions of B and x nuclei in the (A + p) and (y + p) channels; $\sigma^{\mathrm{DW}}(\ldots)$ is the reduced DCS, calculated within the framework of the "usual" DWBA; the values $b_{\mathrm{B}\to\mathrm{A}+p}$ and $b_{x\to y+p}$ are the single-particle ANCs for the shell-model wave functions of the two-body B = (A$+p$) and $x=(y+p)$ bound states, which determine the amplitudes of their tails; E is the relative kinetic energy of the colliding particles, and θ is the center-of-mass scattering angle; the value $\lambda=C^2_{\mathrm{B}\to\mathrm{A}+p;\ell j-}/C^2_{\mathrm{B}\to\mathrm{A}+p;\ell j+}$ is introduced if the total moment of the transferred proton j can have two values: $j^{\pm}=\ell\pm1/2$ and $\lambda=0$ if j takes only one value. In our case, A≡^{11}B, x≡^{10}B, and y≡^{9}Be (B≡^{12}C).

The ANC $C^2_{^{12}\mathrm{C}\to^{11}\mathrm{B}+p}(=C^2_{111}$ in the following notation) should be extracted from Eqs. (1) and (2) by normalizing the calculated DCS to the experimental one in the region of the main maximum of angular distribution. The unknown values of the single particle ANCs $b_{^{12}\mathrm{C}\to^{11}\mathrm{B}+p}(=b_{111})$ and $b_{^{10}\mathrm{B}\to^{9}\mathrm{Be}+p}(=b_{91})$ are calculated as solutions of the appropriate Schrödinger equations taking into account the experimental binding energies. Also, one should know the ANC value for ^{9}Be $+p\to^{10}\mathrm{B}_{\mathrm{g.s.}}$. We used here the "indirectly determined" value of the ANC, namely $C^2_{^{10}\mathrm{B}\to^{9}\mathrm{Be}+p}(=C^2_{91})=4.35\pm0.39$ fm^{-1} [8,24,25] for ^{9}Be $+$ $p\to^{10}$B, the correctness of which was also discussed in [7]. In this case, the calculated value of b^2_{91} has a value equal to 10.92 fm^{-1} at the "standard" values of the geometric parameters of the Woods-Saxon (WS) proton binding potential in the ground state of ^{9}Be.

As noted above, the ANC can be correctly extracted from the experimental data by the MDWBA method only if proton transfer is a peripheral process. For this purpose, in Eq. (1) for the DCS, the function $R(E,\theta;b_{x\to y+p},b_{\mathrm{B}\to\mathrm{A}+p})$ is allocated, which serves as a peripherality test. The value of $R(E,\theta;b_{x\to y+p},b_{\mathrm{B}\to\mathrm{A}+p})=R(b_{\mathrm{B}\to\mathrm{A}+p})$ at fixed values of E, θ, $b_{x\to y+p}$ should remain constant for a peripheral proton transfer process when varying the geometric parameters of the corresponding proton binding potential, which determine the values of $b_{\mathrm{B}\to\mathrm{A}+p}$. This means that the ratio $\sigma^{\mathrm{DW}}(\cdots)/b^2_{\mathrm{B}\to\mathrm{A}+p}$ in Eq. (2) is independent on the ambiguity of the geometric parameters of the B={A + p} binding potential, i.e. on the inner part of the nucleus and provides the same independence for the extracted ANC value.

One notes that in the general case, the spectroscopic factor ($Z_{\mathrm{B}\to\mathrm{A}+a}$), which is the norm of the radial overlap integral of the bound state wave functions of nuclei B = (A + p) and A, is related to the ANC $C_{\mathrm{B}\to\mathrm{A}+a}$ by the equation [26]:

$$C_{\mathrm{B}\to\mathrm{A}+a}=Z^{1/2}_{\mathrm{B}\to\mathrm{A}+a}\bullet b_{\mathrm{B}\to\mathrm{A}+a} \quad (3)$$

As is well known, the single-particle ANC $b_{\mathrm{B}\to\mathrm{A}+p}$ of the model wave function for {A + a} bound in the Woods-Saxon nuclear potential strongly varies with geometric parameters variation, and according to Eq. (3) the extracted Z value should have an inversely proportional change if the reaction is peripheral. Thus, the spectroscopic factor becomes a completely model quantity.

Assessment of the reaction peripherality

To assess the peripherality of proton transfer in the region of the main maximum of the angular distribution of the ^{11}B(^{10}B,^{9}Be)^{12}B reaction, the range of values of the $R(b_{\mathrm{B}\to\mathrm{A}+p})$ function were estimated for each reaction channel under consideration.

Assuming a mechanism of simple proton stripping occurring at the periphery of the interacting nuclei A and x, we can find the so-called "indirectly determined" value (as opposed to the theoretical value) for the squared ANC, $C^2_{\mathrm{B}\to\mathrm{A}+p}$, by normalizing the calculated cross sections to the experimental ones. Typically, the simple stripping mechanism dominates in the region of the main diffraction maximum of the angular distributions of the emitted particles, where it is advisable to normalize the calculations to the experiment. Therefore, it is useful to consider the behavior of the R function in this angular interval. To do this, we analyze the behavior of the test function in the form [27,28]:

$$\rho(b_{\mathrm{B}\to\mathrm{A}+p})=R(b_{\mathrm{B}\to\mathrm{A}+p})/R_0(b_{\mathrm{B}\to\mathrm{A}+p}) \quad (4)$$

where $R_0(b_{\mathrm{B}\to\mathrm{A}+p})$ is calculated at "standard" values of the geometric parameters ($r_0=1.25$ fm and $a=0.65$ fm) of the bound state potential {B→A + p}. In this case, an array of values of the test function $\rho(b_{\mathrm{B}\to\mathrm{A}+p})$ is considered for pairs of geometric parameters for all angles in the region of the main maximum. Before analyzing the experimental DCSs to obtain the ANC, we determine the ranges of the test functions $\rho(b=b_{11\,1}(r_0,a))$ proton transfer to the ground (0^+), first (4.44 MeV, 2^+) and third (9.64 MeV, 3^-) excited states of the ^{12}C nuclei, which are designated as $\rho_{11\,1^{(0)}}$, $\rho_{11\,1^{(1)}}$ and $\rho_{11\,1^{(3)}}$.

Calculations of the single particle DCS $\sigma^{\mathrm{DW}}(\cdots)$ in Eq. (2), were carried out using the DWUCK5 code of the Nuclear Reaction Video (NRV) program [29].

The optical potentials were taken at conventional form as used in Ref. [14] with WS form factors (without the spin-orbital term), and the Coulomb potential is of a spherical, uniform charge distribution of radius R_{C}. The imaginary part includes only the volume term.

Six sets of optical potentials (OPs) listed in Table 1 were used for the calculations. The OP parameters for the entrance channel are taken from our work on the ^{11}B+^{10}B elastic scattering [14] at the beam energy of 41.3 MeV.

The cross sections we measured were analyzed simultaneously with other available data on reaction and scattering using the FRESCO program [30] upgraded with χ^2 minimization SFRESCO code [31] to get the optimal potential parameters. Also, the OP parameters obtained in Ref. [32] were used, in which the energy of the ^{10}B ion beam ($E_{10_B}=40$ MeV) is very close to that in our experiment.

For the OP parameters of the exit channel, we utilize from our previous works [8,16] and from the database of the online DWBA program NRV [29].

The variation of $b_{11\,1}(r_0,a)$ values was realized by solving the Schrödinger equation with different pairs of geometric parameters of the nuclear part in the WS form of the $^{12}\mathrm{C}\to^{11}\mathrm{B}+p$ bound state potential, which also contains Coulomb and spin–orbit terms. The geometric parameters were varied within the physically acceptable limits of $1.1\le r_0\le1.4$ fm and $0.5\le a\le0.8$ fm. Such variation of r_0 and a results in changing the single-particle ANCs, $b_{11\,1}$, in the interval of $6.80\le b_{11\,1^{(0)}}\le13.90$ fm$^{-1/2}$ for the ground state, $4.40\le b_{111^{(1)}}\le8.99$ fm$^{-1/2}$ for the 1st excited (4.44 MeV, 2^+) state and $1.42\le b_{11\,1^{(3)}}\le3.02$ fm$^{-1/2}$ for the 3rd excited (9.64 MeV, 3^-) state.

Fig. 4 shows plots of the $\rho(b_{11\,1})$ dependences on the single-particle ANCs, $b_{11\,1}$, in the ground (0^+), 1st (2^+) and 3rd (3^-) excited states of the ^{12}C nucleus at $\theta_{\mathrm{cm}}=11^\circ$ when the OP set "A1 + B1" from Table 1 was used.

The spread of values of $\rho(b)$ at a certain angle is the result of the weak "residual" dependence of R to changes in the parameters r_0 and a when $b_{111}(r_0,a)=\mathrm{const}$ [33]. For example, $\rho(b_{11\,1})$ changes within the intervals of $0.96\le\rho(\theta;b_{11\,1^{(0)}})\le1.02$ for the ground state, $0.92\le\rho(\theta;b_{11\,1^{(1)}})\le1.07$ for the 1st excited state, and $0.95\le\rho(\theta;b_{11\,1^{(3)}})\le1.03$ for the 3rd excited states of the ^{12}C nucleus at $\theta_{\mathrm{cm}}=11^\circ$, respectively.

In general, for the functions $\rho(b_{11\,1})$ averaged over angles, used to obtain the ANC, their values change within the limits of ±2.8%, ±7.2% and ±3.9% for the proton transfer to the ground, first and third excited states of the nucleus ^{12}C, respectively. It follows that the function ρ has a

Table 1
Parameters of the optical potentials for the entrance (A) and exit (B) channels for the ^{11}B(^{10}B,^{9}Be)^{12}C reaction at $E_{^{10}B} = 41.3$ MeV.

Channel	OP	V_RMeV	$r_R$fm	$a_R$fm	W_0MeV	$r_W$fm	$a_W$fm	$r_C$fm	Ref.
^{10}B+^{11}B	A1	69.705	2.282	0.462	40.330	2.282	0.462	2.56	[32]
	A2	97.034	2.312	0.414	13.601	2.461	0.414	2.56	[32]
	A3	75.46	2.282	0.390	12.17	2.282	0.800	2.461	[14]
^{9}Be+^{12}C	B1	100	2.195	0.428	15	2.481	0.248	2.386	[8,16]
(^{10}B+^{12}C)	B2	66.31	2.271	0.429	27	2.405	0.285	2.386	[8,16]
	B3	78.63	2.244	0.429	37.8	2.378	0.285	2.386	[8,29]

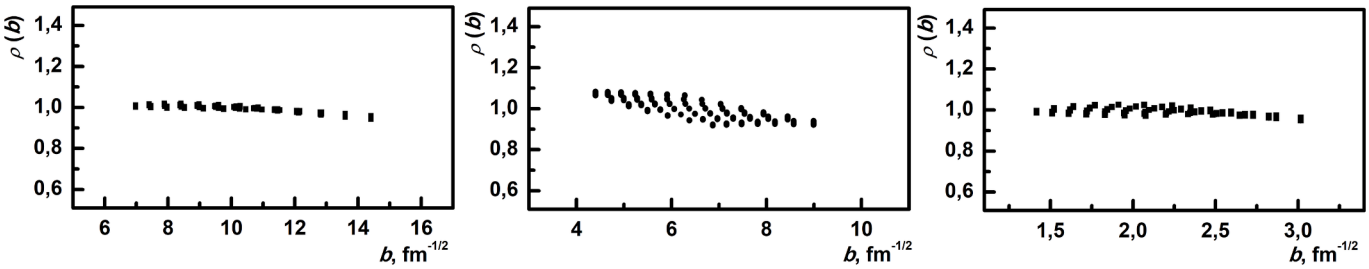

Fig. 4. Dependences of $\rho(b_{11\,1})$ on the single-particle ANCs $b_{11\,1}$ for the reaction ^{11}B(^{10}B,^{9}Be)^{12}C at $\theta_{cm} = 11^{\circ}$ and the nucleus ^{12}C at the ground (0^+) and excited (2^+) and (3^-) states calculated with the OP set "A1 + B1" in Table 1.

rather weak dependence on the variation of the geometric parameters, and these ranges do not exceed the experimental errors of the DCSs. Hence, these channels of the reaction are practically peripheral in the regions of the main maxima of the angular distribution.

Interfering reactions with other mechanisms

When extracting the ANC value from the normalization of the calculated DCS to the experiment, it is assumed that the reaction proceeds predominantly through a one-step proton transfer on the nuclear surface. Also, since the energy resolution of the ΔE detector did not allow reliable separation of the detected beryllium isotopes, the possibility of the contribution of other reactions with the formation of $^{7\text{-}11}$Be nuclei, shown in the diagrams in Fig. 5, was analyzed. The series of diagrams show the most probable mechanisms of the processes leading to the formation of other beryllium isotopes registered in the same locus of the two-dimensional spectrum. This could, in principle, lead to interference of the corresponding events with the events from the considered ^{11}B(^{10}B, ^{9}Be)^{12}C reaction.

The ^{8}Be nucleus (diagram 2) in the ground state decays into two α-particles ($\Gamma_{tot} = 6.8$ eV), and cannot be detected. The reaction with the formation of ^{10}Be proceeds through the charge-exchange mechanism (diagram (4′)) or through the proton transfer mechanism (diagram 4″). The energy of the ^{10}Be group in the spectra of recorded beryllium nuclei is ~ 2 MeV lower than the energy of the ^{9}Be group corresponding to the excitation of the level at E^*= 9.64 MeV (3^-) of the ^{12}C nucleus ($Q = -0.28$ MeV) for the reaction of interest to us (diagram 3). So only ^{7}Be in the ground state (diagram 1) can in principle interfere with the ^{9}Be level with an excitation energy of 9.64 MeV. However, in the region of the forward angles, the energy of the ^{7}Be nuclei is ~ 2 MeV higher, and at our experimental resolution (see Fig. 2), there is no overlap.

The remaining diagram 5 shows another direct mechanism (leading to the formation of "target-like" ^{9}Be nucleus). But the DCS of which should be relatively small in the region of the forward angles. The evaluation of contribution of this mechanism to the DCS of the ^{11}B (^{10}B,^{9}Be)^{12}C reaction with DWBA calculations shows its negligible value (see section 3.4).

Since the procedure of ANC extraction assumes that the reaction mechanism is direct and single-step in the angular region where the calculated DCS are normalized to the experimental values, we also estimated the possible contribution of the compound nucleus mechanism in this region of the main maximum of the angular distribution. At that, an assumption was made about the symmetry of its contribution in the forward and backward hemispheres of the emission angles of the reaction products. Our estimates show that this contribution to the DCS of the reaction at small angles does not exceed 15 %, which is significantly less than the overall uncertainties of extracted ANC values.

Obtaining the ANC squares

As noted above, calculations of the DCSs of the ^{11}B(^{10}B,^{9}Be)^{12}C reaction with population of the ground (0^+) and excited states at E^*=4.44 MeV (2^+) and E^*=9.64 MeV (3^-) were carried out in accordance with Eqs. (2) and (3). Under the assumptions made, the normalization of the calculated DCS in the region of small angles is determined by the product of the squares of the corresponding ANC, and the values of the squares of the ANC C^2_{111} for proton binding in the indicated states of the ^{12}C nucleus were determined taking into account the known value of $C^2_{9\,1}$ (= 4.35 fm^{-1}). Calculations were done for all sets of the optical potentials of Table 1. As the proton transfer is peripheral in all cases, the wave functions of the bound states were calculated with a WS potential with geometric parameters $r_0 = 1.25$ fm and $a = 0.65$ fm. The values of the orbital and total angular moments of the transferred proton were taken as $p_{3/2}$ in 0^+, $p_{1/2}$ and $d_{5/2}$ in 2^+ and 3^- states of ^{12}C, respectively.

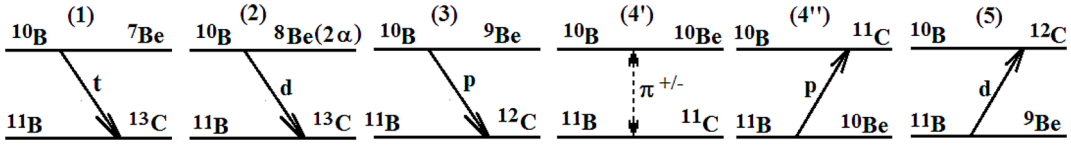

Fig. 5. Diagrams of processes leading to the formation of Be isotopes in ^{11}B+^{10}B interaction.

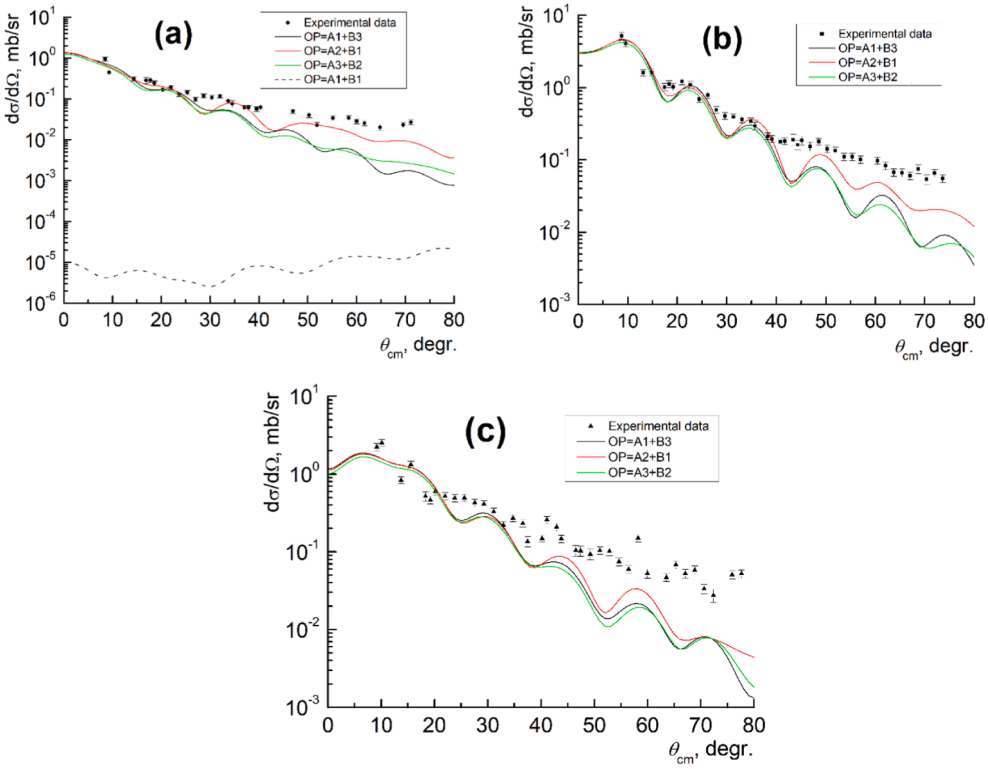

Comparison of calculated angular distributions of DCSs with experimental data for the ^{11}B(^{10}B,^{9}Be)^{12}C reaction with transitions (a) - to the ground state (0^+), (b) - E^*=4.44 MeV (2^+) and (c) - E^*=9.64 MeV (3^-) excited states.

Fig. 6. Comparison of calculated angular distributions of dcss with experimental data for the^{11}B(^{10}B,^{9}Be)^{12}C reaction with transitions (a) – to the ground state (0^+), (b) – E^*=4.44 MeV (2^+) and (c) – E^*=9.64 MeV (3^-) excited states.

Fig. 6 shows a comparison of the experimental angular distributions of the DCS with the calculated ones for the three best sets of OPs, which in each case are normalized by the least squares method to the 4–5 most forward experimental points. It is seen that the behavior of calculated DCSs is in satisfactory agreement with the experimental data within the main maximum of the angular distribution and up to 40°, but the calculations underestimate DCSs at large angles for all sets of optical potentials. Obviously, the reason for this is the increase in the contribution of other more complex mechanisms to the reaction cross section with increasing angle. A similar situation was observed in the reaction ^{12}C (^{10}B,^{9}Be)^{13}N, studied at the same energy [8]. The dotted curve in Fig. 6a demonstrates the order of the absolute value of the DCS for the process of deuteron pickup (see diagram 5 in Fig. 5). The curve was calculated within the framework of DWBA with OP set "A1 + B1" under the assumption that the spectroscopic factors of the configurations ^{11}B=$\{^{9}$Be + $d\}$ and ^{12}C=$\{^{10}$B + $d\}$ are equal to unity. It is obvious that the contribution of this process to the DCS reaction in the region of small angles is negligible for any reasonable values of spectroscopic factors. The same argument applies to the other two reaction channels.

From the normalization coefficients, the values of ANC squares corresponding to different sets of OPs were obtained and averaged over them. The resulting values of the squares ANC are$C^2_{11\ 1^{(0)}} = 322 \pm 76$ fm$^{-1} = 322 \pm 64.4$(exp) $\pm$ 40.4(*th*) fm^{-1}, $C^2_{11\ 1^{(1)}}$=32.8 $\pm$ 8.4 fm^{-1} = 32.8 $\pm$ 6.2(exp) $\pm$ 5.6 (*th*) fm^{-1} and $C^2_{11\ 1^{(3)}} = 1.26 \pm 0.44$ fm$^{-1} = 1.26$ $\pm$ 0.26(exp) $\pm$ 0.35(*th*) fm^{-1}. The experimental part (exp) is the sum of the experimental DCS errors (10 –12%) and the systematic uncertainty in the $C^2_{9\ 1}$ value (9 %). The theoretical part (*th*) represents the root-mean-square values of the ambiguity of the OP parameters (12 %, 15 %, 27 % for the ground, first and third excited states of the ^{12}C nucleus, respectively) and the uncertainties due to the "residual" dependence of the $R(\ldots)$ functions (~3 %, ~7 %, ~4 % for the ground, first and third excited states of the ^{12}C nucleus, respectively). In this case, the main error is the scatter in the values of the normalization coefficient for different experimental points of the DCS, which in some cases reaches 25%. The corresponding scatter in the experimental DCS values relative to the DWBA calculating curves is not entirely clear, since the experimental errors are significantly smaller (10–12 %).

As it was mentioned at Introduction, we did not find in the literature the values of the "indirectly measured" ANC for the bound states of the proton in the ^{12}C nucleus that we considered, with the exception of our old work [8]. The ANC values $C^2_{11\ 1^{(0)}} = 223 \pm 31$ fm^{-1}, $C^2_{11\ 1^{(1)}} = 15.8 \pm$ 3.5 fm^{-1} and $C^2_{11\ 1^{(3)}} = 0.58 \pm 0.11$ fm^{-1} found in Ref. [9] are significantly less than those determined in this work. One of the reasons for such discrepancy can be the fact that the proton stripping into lower tightly bound states turned out to be not peripheral in the reaction ^{11}B (^{3}He, d)^{12}C. However, theoretical estimates of the ANC value $C^2_{11\ 1^{(0)}} =$ 199 fm^{-1}, made in Refs. [34,35] within the framework of the Source Term Approach [35] shows satisfactory agreement with the value obtained in Ref. [9]. Obviously, in the future it is necessary to analyze more thoroughly the available experimental data on proton transfer to the states of the ^{12}C nucleus.

Astrophysical *S*-factor and reaction rate of the ^{11}B(p, γ)^{12}C reaction

The calculation of the astrophysical *S*-factor of the ^{11}B(p, γ)^{12}C radiative capture reaction was carried out within the framework of the modified *R*-matrix method, previously successfully used to analyze a number of reactions [10–13]. Calculations were carried out for transitions to the ground state (0^+) and 1-st exited state at $E^* = 4.44$ MeV (2^+)

of the ^{12}C nucleus since the experimental data are available only for these transitions. The observed partial and total resonance widths with their exact energy dependence, as well as experimental ANC values obtained in the previous section were utilized.

Modified R-matrix method

In this section, we provide explicit expressions for determining the astrophysical *S*-factor for the reaction ^{11}B$(p,\gamma)^{12}$C within the framework of the modified *R*-matrix method. According to the standard definition, the astrophysical *S*-factor is determined by the following expression:

$$S(E) = Ee^{2\pi\eta}\sigma(E) \tag{5}$$

where σ(*E*) is the radiative capture cross section, *E* is the relative kinetic energy of colliding particles ^{11}B and *p*, and η is the Sommerfeld parameter.

The total cross section σ(*E*) for the process of radiative capture into the ground and excited states of the ^{12}C nucleus with spin J_f is defined as

$$\sigma(E) = \sum_{J_f J_i} \sigma_{J_f J_i}(E) \tag{6}$$

Here J_i is the total angular momentum of the $^{11}\mathrm{B} + p$ system and

$$\sigma_{J_f J_i}(E) = \frac{\pi}{4k^2}\sum_{Il_iJ_iL}(2J_i+1)\left|M_{Il_iJ_iJ_fL}\right|^2 \tag{7}$$

where I and l_i are the spin and relative orbital momentum of the entrance channel, respectively, L is the multipolarity of the electromagnetic transition, $k^2 = 2\mu E$ and μ is the reduced mass of the $^{11}\mathrm{B} + p$ system. $M_{Il_iJ_iJ_fL}$ is amplitude of the transition from the initial state (I,l_i,J_i) to the final state (J_f,I,L), which consists of two parts: resonant $M^{(R)}_{Il_iJ_iJ_fL}$ and direct $M^{Dir}_{Il_iJ_iJ_fL}$ capture. In the single-level approximation, the amplitude $M^{(R)}_{Il_iJ_iJ_fL}$ of the resonant capture can be represented as [10–13]:

$$M^{(R)}_{Il_iJ_iJ_fL} = ie^{(\varpi_{l_i}-\delta_{l_i})}\frac{\left[\Gamma^{(p)}_{Il_iJ_i}(E)\right]^{1/2}\left[\Gamma^{(\gamma)}_{J_iJ_fL}(E)\right]^{1/2}}{E - E^{(R)}_{J_i} + i\frac{\Gamma_{J_i}}{2}} \tag{8}$$

Here ϖ_{l_i} and δ_{l_i} are the Coulomb and hard-sphere phase shifts for ^{11}B-*p* scattering, respectively. Γ_{J_i} is full width of the resonant state $(E^{(R)}_{J_i}; J_i)$, which is defined as the sum of the widths of all allowed decay channels of the state, including proton $(\Gamma^{(p)}_{J_i})$, α-particle $(\Gamma^{(\alpha)}_{J_i})$ and radiative $\Gamma^{(\gamma)}_{J_i}$ decay channels. The partial proton and radiation widths are defined by the following expressions [10–13]:

$$\Gamma^{(p)}_{Il_iJ_i}(E) = \frac{2P_{l_i}(E)\left(\gamma^{(p)}_{Il_iJ_i}\right)^2}{1 + \left(\gamma_{Il_iJ_i}\right)^2\left(\frac{dS_c}{dE}\right)_{E=E^{(R)}_{J_i}}} \tag{9}$$

$$\Gamma^{(\gamma)}_{J_iJ_fL}(E) = \frac{2k_\gamma^{2L+1}\left(\gamma^{(\gamma)}_{J_iJ_fL}\right)^2}{1 + \left(\gamma_{Il_iJ_i}\right)^2\left(\frac{dS_c}{dE}\right)_{E=E^{(R)}_{J_i}}} \tag{10}$$

where k_γ is the photon momentum, P_{l_i} is the barrier penetration factor, $\left(\frac{dS_c}{dE}\right)_{E=E^{(R)}_{J_i}}$ is the energy derivative of the shift factor at the resonance energy, and $\gamma^{(p)}_{Il_iJ_i}$, $\gamma^{(\gamma)}_{J_iJ_fL}$ are the sum of amplitudes of the reduced proton and radiative widths, respectively. $\gamma_{Il_iJ_i} = \sum_\lambda \gamma^{(\lambda)}_{Il_iJ_i}$ is the sum of the amplitudes of the reduced widths of open channels, r_C is the channel radius, which is the distance of the simultaneous transition of the radial wave functions of the initial and final states to their asymptotics.

According to the long-wave approximation [10] the direct capture amplitude $M^{Dir}_{Il_iJ_iJ_fL}$ for *EL*- and *M*1-multipole transitions are given by the expressions

$$M^{Dir,EL}_{Il_iJ_iJ_fL} = i^{l_i+L-l_f}\sqrt{\frac{2\mu}{k}}k_\gamma^{L+1/2}\mu^L\left[\frac{Z_p}{m_p^L} + (-1)^L\frac{Z_B}{m_B^L}\right]\left[\frac{(L+1)(2L+1)}{L}\right]^{1/2}$$

$$\times\frac{1}{(2L+1)!!}C^{J_f0}_{l_i0L0}\sqrt{(2l_i+1)(2J_f+1)}W(Ll_fJ_iI;l_iJ_f) \tag{11}$$

$$\times C_{l_fI}\int_{r_c}^{\infty} drr^L W_{-\eta_{pB},l_f+1/2}(2\chi_{pB}r)\left[I_{l_i}(r) - e^{2i(\varpi_{l_i}-\delta_{l_i})}O_{l_i}(r)\right]$$

$$M^{Dir,M1}_{Il_iJ_iJ_f} = -2ie^{i(\varpi_{l_i}-\delta_{l_i})}\sqrt{\frac{\mu}{3k}}k_\gamma^{3/2}\frac{e}{m}W(1IJ_fl_i;IJ_f)$$

$$\times\left[W(1S_pIS_B;J_pI)\sqrt{\frac{J_p+1}{J_p}}\mu_p + W(1J_BIJ_B;J_pI)\sqrt{\frac{S_B+1}{S_B}}\mu_B\right]$$

$$\times C_{l_fI}\int_{r_c}^{\infty} drW_{-\eta_f,l_f+1/2}(2\chi r)\left[I_{l_i}(r) - e^{2i(\varpi_{l_i}-\delta_{l_i})}O_{l_i}(r)\right] \tag{12}$$

where $I_{l_i}(r)(O_{l_i}(r))$ is the incoming (outgoing) Coulomb wave function of *p*A scattering, $\lambda_p = \hbar/m_pc = 0.2103$ fm is the Compton wavelength of proton, $W_{\alpha:\beta}(x)$ is the Whittaker function, $C^{l_30}_{l_10l_20}$ is the Clebsch–Gordon coefficient, $W(abcd:ef)$ is the Racah coefficient and $C_{l_fI} = C_{11\,1}$ is the ANC of the state of ^{12}C nucleus in the bound $^{11}\mathrm{B} + \mathrm{p}$ configuration. Note that the amplitude of direct radiative capture is normalized through the ANC C_{l_fI}. This makes it possible to fix the contribution of the amplitude of the direct part, which facilitates the process of adjusting the resonant widths.

The amplitude of the reduced radiation width consists of two parts-internal and external ones [36,37]:

$$\gamma^{(\gamma)}_{J_iJ_fL} = \gamma^{(\gamma)}_{J_iJ_fL}(int) + \gamma^{(\gamma)}_{J_iJ_fL}(ext), \tag{13}$$

where

$$\gamma^{(\gamma)}_{J_iJ_fL}(ext) = i^{l_i+L-l_f}e^{i(\varpi_{l_i}-\delta_{l_i})}\gamma^{(a)}_{Il_iJ_i}\sqrt{\frac{2\mu}{k_i}}\mu^L\left[\frac{Z_p}{m_p^L} + (-1)^L\frac{Z_B}{m_B^L}\right]\left[\frac{(L+1)(2L+1)}{L}\right]^{1/2}$$

$$\times\frac{1}{(2L+1)!!}C^{J_f0}_{l_i0L0}\sqrt{(2l_i+1)(2J_f+1)}W(Ll_fJ_iI;l_iJ_f)$$

$$\times C_{l_fI}\int_{r_c}^{\infty} drr^L W_{-\eta_{pB},l_f+1/2}(2\chi_{pB}r)O_{l_i}(r) \tag{14}$$

It is clear that the reduced external radiation width $\gamma^{(\gamma)}_{J_iJ_fL}(ext)$ is directly dependent on the reduced partial width $\gamma^{(p)}_{Il_iJ_i}$ and ANC. Such dependence gives some advantage when adjusting the value of the radiation width using Eq. (8).

The fact is that in the fitting process only the value $\gamma^{(\gamma)}_{J_iJ_fL}(int)$ will vary, while $\gamma^{(\gamma)}_{J_iJ_fL}(ext)$ will be fixed. It is worth noting that an accurate calculation of the energy dependence of the radiation width using Eqs. (11) and (12) allows one to extrapolate correctly the resonant tail in the region of ultra-low astrophysically important energies.

Thus, using the modified *R*-matrix method will make it possible to calculate the astrophysical *S*-factor of radiative capture reactions occurring through the formation of intermediate states with correct consideration of the contributions of both resonant and direct radiative capture. At that, the contribution of the direct radiation amplitude is fixed using the known ANC value.

Results of calculating the astrophysical $S-$ factor of the $^{11}B(p,\gamma)^{12}C$ reaction

The radiative decay of the resonance states 16.10 (2^+), 16.57 (2^-) and 17.23 MeV (1^-), into the ground (0^+) (γ_0-transitions) and first excited 4.44 MeV (2^+) (γ_1-transitions) states were taken into account in the calculations.

The input parameters necessary for calculating the astrophysical S-factor (proton, alpha and radiation widths, total widths) in addition to the ANC values we found, were taken from Ref. [37]. The experimental values of the astrophysical S-factor were taken from Refs. [6,37–40].

The χ^2 method was used as a tool for fitting to the experimental data. The ANCs obtained in the work for the ground and first excited states of the ^{12}C nucleus were taken as fixed values. As a result, almost all adjustable resonant widths were kept practically unchanged or changed within the error limits given in the original source.

The exceptions were radiative transitions from the 3rd resonance state to the ground state and from the 2nd resonance state to the 1st excited state of the ^{12}C nucleus. The best agreement with the experimental values of S-factors was achieved with radiation widths equal to: $\Gamma_{J_i}^{(\gamma_0)} = 30.0 \pm 3.0$ eV and $\Gamma_{J_i}^{(\gamma_1)} = 6.0 \pm 1.0$ eV versus the values of 40 eV and 8 eV used in Ref. [37] respectively.

The used values of these quantities are given in Table 2.

The results of calculations of the astrophysical S-factors of the transitions to the ground (0^+) and 1st excited (2^+) states in the $^{11}B(p,\gamma)^{12}C$ reaction, as well as their sum are shown in Fig. 7. The dashed line represents the transitions to the (2^+) state (γ_1-transitions), the solid green line demonstrates γ_0-transitions and the solid black line is the summed ($\gamma_0 + \gamma_1$) astrophysical S-factor. The dash dotted line represents the contribution of direct radiative capture to γ_1 transitions. The contribution of direct radiative capture to γ_0 transitions turned out to be 2–3 times weaker than the similar contribution to γ_1-transitions. In Fig. 7 the direct radiative capture to γ_0 transitions is not presented.

As can be seen from Fig. 7, the calculated values of the astrophysical S-factor are in good agreement with the available experimental data. Despite the fact that the amplitudes of direct radiative captures are significantly smaller than the amplitude of resonant capture to the first resonant state, the role of direct captures becomes sufficient and ensures the almost horizontal behavior of the astrophysical S-factor below the resonance. This occurs due to constructive interference of resonant and direct amplitudes in the low energy region.

The values of the astrophysical S-factors of the $^{11}B(p,\gamma)^{12}C$ reaction at $E = 0$ were determined to be equal to: for γ_0 transitions $S(0,\gamma_0) = 1.77 \pm 0.27$ keV·b; for γ_1 transitions – $S(0,\gamma_1) = 1.23 \pm 0.20$ keV·b. These values are in excellent agreement with the values of 2.0 ± 0.4 keV·b and 1.3 ± 0.3 keV·b obtained in [38]. The summed value of the astrophysical S-factor was determined to be $S(0) = 3.00 \pm 0.45$ keV·b ($S^{dir}(0) = 0.360$ keV·b).

The found value of $S(0,\gamma_0)$ is also in excellent agreement with the estimate of 1.8 ± 0.4 keV·b in [39], while $S(0,\gamma_1)$ is almost 3 times less than the value of 3.5 ± 0.6 keV·b, obtained there. Such difference in the values of the astrophysical S-factors can be understandable as follows: as

Table 2
Values of the resonance widths used in the calculation of the astrophysical S-factor of the reaction $^{11}B(p,\gamma)^{12}C$.

N№	E_{res} (keV) (J_i^π)	Γ_{J_i}(keV)	$\Gamma_{J_i}^{(p)}$(keV)	$\Gamma_{J_i}^{(\gamma_0)}$(eV)	$\Gamma_{J_i}^{(\gamma_1)}$(eV)
1	163 (2^+)	5.3 ± 0.2	0.0215 ± 0.0033	0.59 ± 0.11	12.8 ± 1.5
2	675 (2^-)	300	150	not taken into account	6.0 ± 1.0 (this work)
3	1388 (1^-)	1150	1000	30.0 ± 3.0 (this work)	5

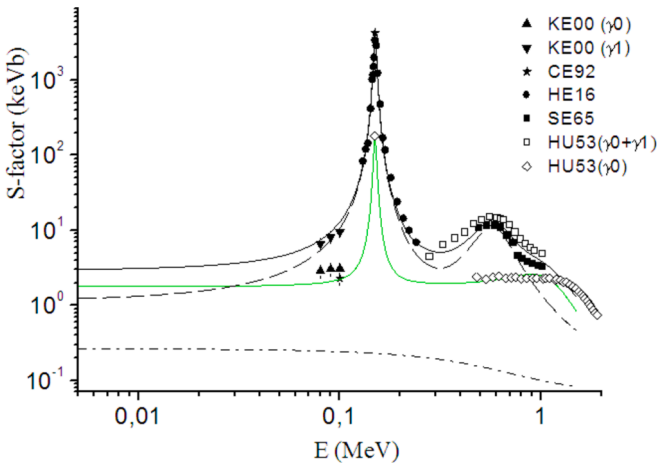

Fig. 7. Astrophysical S-factors of γ_0-, γ_1-transitions and total ($\gamma_0 + \gamma_1$) astrophysical S-factor in the $^{11}B(p,\gamma)^{12}C$ reaction.

can be seen from Fig. 3 in Ref. [39], the calculated value of the astrophysical S-factor for γ_1-transitions directly in the resonance region are not substantiated by any experimental data. As a result, the calculated curve passes slightly touching the upper values of the three existing experimental points, while our calculations are well supported by both "peak" and "tail" experimental points. It is worth noting how accurately the height of the experimental peak values from Refs. [38] and [40] is reproduced by changing the radiation widths $\Gamma_{J_i}^{(\gamma_0)}$ and $\Gamma_{J_i}^{(\gamma_1)}$.

Thus, within the framework of the modified R-matrix method, an analysis of the experimental data on the astrophysical S-factor of the reaction $^{11}B(p,\gamma)^{12}C$ in the energy range $E \leq 1.5$ MeV was carried out, one of the advantages of which is the possibility to utilize directly the ANC value to fix the contribution of direct radiative capture. Such approach to analysis significantly simplified and improved the process of tuning the width of the resonances. As a result of the analysis, new values of the radiation widths $\Gamma_{J_i}^{(\gamma_0)}$ and $\Gamma_{J_i}^{(\gamma_1)}$ were determined, which made it possible to accurately normalize the peak heights to the existing experimental data.

As a whole, a good description of the experimental data was achieved both in the region of resonance energies and outside the region of resonances. The obtained new values of astrophysical S-factors at zero energy are in excellent agreement with the literature data. Nevertheless, it is obvious that the additional precise measurement of the experimental values of the cross section (astrophysical S-factor) of the $^{11}B(p,\gamma)^{12}C$ reaction in the energy region $E < 100$ keV is necessary.

The rate of the reaction $^{11}B(p,\gamma)^{12}C$

This section presents the results of calculating the $^{11}B(p,\gamma)^{12}C$ reaction rate, based on the energy dependence of the astrophysical S-factor obtained in the previous section for the reaction proceeding through the γ_0- and γ_1-transitions.

To calculate the reaction rate, a generally accepted expression was used, obtained under the assumption that particles in the stellar medium have a Maxwellian velocity distribution. According to the latter, the reaction rate averaged over particles is determined by the following expression [41]:

$$N_A < \sigma\vartheta >= N_A \frac{(8/\pi)^{1/2}}{\mu^{1/2}(k_B T)^{3/2}} \int_0^\infty E\sigma(E)\exp[-E/(k_B T)]dE \qquad (15)$$

where N_A is Avogadro number, $\sigma(E)$ is the reaction cross section at the proton-projectile energy E. k_B is Boltzmann constant and T is the temperature.

When the astrophysical *S*-factor is assumed to be a constant, the integrand in Eq. (15) is peaked at the energy the "most effective energy" (Gamow energy) [42]

$$E_0 = \left(\frac{\mu}{2}\right)^{1/3}\left(\frac{\pi e^2 Z_1 Z_2 k_B T}{\hbar}\right) \quad (16)$$

where Z_1 and Z_2 are charges of the colliding particles. In our case, the latter are ^{11}B and proton. Since the astrophysical *S*-factor obtained by us is a fairly smooth function, with the exception of the first resonance, expression (16) can be used as an approximate energy corresponding to the temperature of the medium.

Fig. 8 presents the results of calculations of the ^{11}B(p,γ)^{12}C reaction rates for the γ_0- and γ_1- transitions, indicated by red and blue curves, respectively, and the total reaction rate, indicated in black. As shown in the inset to Fig. 8, the priorities of the contributions of the γ_0- and γ_1-transitions to the reaction rate change with increasing temperature in accordance with the energy behavior of the corresponding astrophysical *S*-factors for each of the transitions (see Fig. 7). Calculations have shown that at low temperatures, up to $T_9 \sim 0.02$–0.03 K (periphery of the star), the process of formation of ^{12}C nuclides in the ground state predominates, while at temperatures above $T_9 = 0.03$ K (interior of the star), the process of formation of ^{12}C in the first excited state begins to dominate.

Fig. 9 shows the ratio of the calculated reaction rates to those established in the review work [41]. The gray band corresponds to the limit of possible values of the reaction rate associated with the uncertainty of the astrophysical *S*-factor values we obtained.

As can be seen from the Fig. 9, our results are in good agreement with the data of Ref. [41]. In particular, in the region of resonances 163 keV (2^+) and 675 keV (2^-), corresponding $T_9 = 0.1$–1 K, they agree very well. This is explained by the fact that the total astrophysical *S*-factors obtained both in this work and in Ref. [41] are very similar in describing the shape of these resonances, including their heights.

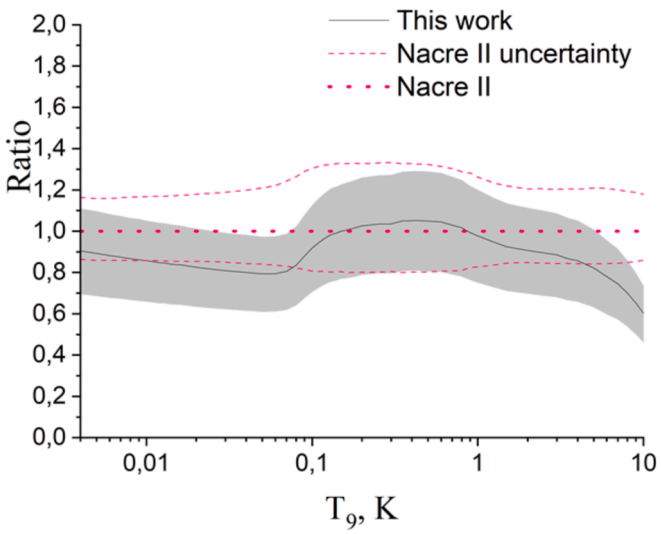

Fig. 9. ^{11}B(p,γ)^{12}C reaction rates in units of the NACRE II (adopt) values.

The predominance of the ^{11}B(p,γ)^{12}C reaction rate values established in [41] in the low-energy region (the region to the left of the peak) relative to our values is a consequence of the prevailing values of the astrophysical *S*-factor in the energy region under consideration. In particular, in Ref. [41] the value of the astrophysical *S*-factor was obtained $S(0) = 4.3^{+0.8}_{-0.6}$ keV·b, while our value is $S(0) = 3.0 \pm 0.67$ keV·b.

Also, a discrepancy is observed above the temperature $T_9 = 1$ K, where the contribution of capture to higher-energy resonances located above energies E = 2 MeV, which were not taken into account in this

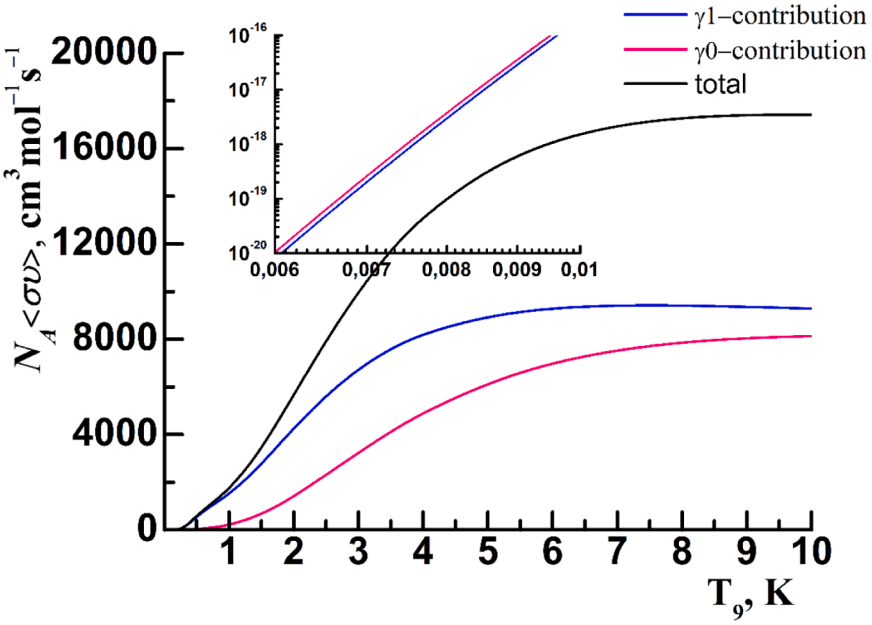

^{11}B(p,γ)^{12}C reaction rate. For clarity of the contribution to the formation of ^{12}C nuclides, the rates of reactions proceeding through the γ_0- and γ_1-transitions are shown separately. Calculations have shown that at low temperatures, up to $T_9 \sim 0.02$–0.03 K the reaction rate dominates through the γ_0 - transitions (the inserted panel), but at higher temperatures it dominates through the γ_1 transitions (the main panel).

Fig. 8. ^{11}B(p,γ)^{12}C reaction rate. For clarity of the contribution to the formation of ^{12}C nuclides, the rates of reactions proceeding through the γ_0- and γ_1-transitions are shown separately. Calculations have shown that at low temperatures, up to $T_9 \sim 0.02$–0.03 K the reaction rate dominates through the γ_0 – transitions (the inserted panel), but at higher temperatures it dominates through the γ_1 transitions (the main panel).

Table 3
$^{11}B(p,\gamma)^{12}C$ reaction rates in [$cm^3mol^{-1}s^{-1}$] units.

T_9, K	The Gamow peak energy, MeV	Adopted reaction rate	Uncertainty	T_9, K	The Gamow peak energy, MeV	Adopted reaction rate	Uncertainty
0.004	0.0189	1.61E-24	3.70E-25	0.16	0.221	1.96E + 00	4.51E-01
0.005	0.0219	3.26E-22	7.50E-23	0.18	0.239	5.37E + 00	1.24E + 00
0.006	0.0248	1.87E-20	4.31E-21	0.2	0.257	1.19E + 01	2.74E + 00
0.007	0.0274	4.75E-19	1.09E-19	0.25	0.298	4.79E + 01	1.10E + 01
0.008	0.03	6.84E-18	1.57E-18	0.3	0.336	1.16E + 02	2.68E + 01
0.009	0.0325	6.52E-17	1.5E-17	0.35	0.373	2.13E + 02	4.90E + 01
0.01	0.0348	4.54E-16	1.04E-16	0.4	0.407	3.28E + 02	7.54E + 01
0.011	0.0371	2.48E-15	5.70E-16	0.45	0.44	4.51E + 02	1.04E + 02
0.012	0.0393	1.11E-14	2.56E-15	0.5	0.473	5.76E + 02	1.33E + 02
0.013	0.0415	4.27E-14	9.81E-15	0.6	0.534	8.18E + 02	1.88E + 02
0.014	0.0436	1.43E-13	3.30E-14	0.7	0.591	1.04E + 03	2.40E + 02
0.015	0.0456	4.31E-13	9.92E-14	0.8	0.646	1.26E + 03	2.91E + 02
0.016	0.0476	1.18E-12	2.71E-13	0.9	0.699	1.49E + 03	3.43E + 02
0.018	0.0515	7.02E-12	1.61E-12	1	0.75	1.74E + 03	4.01E + 02
0.02	0.0553	3.26E-11	7.5E-12	1.25	0.87	2.50E + 03	5.74E + 02
0.025	0.0641	7.10E-10	1.63E-10	1.5	0.983	3.44E + 03	7.91E + 02
0.03	0.0724	7.49E-09	1.72E-09	1.75	1.09	4.52E + 03	1.04E + 03
0.04	0.0877	2.37E-07	5.44E-08	2	1.19	5.66E + 03	1.30E + 03
0.05	0.102	2.84E-06	6.53E-07	2.5	1.38	7.94E + 03	1.83E + 03
0.06	0.115	1.98E-05	4.55E-06	3	1.56	1.00E + 04	2.30E + 03
0.07	0.127	1.03E-04	2.36E-05	3.5	1.73	1.17E + 04	2.70E + 03
0.08	0.139	4.83E-04	1.11E-04	4	1.89	1.32E + 04	3.03E + 03
0.09	0.151	2.20E-03	5.06E-04	5	2.19	1.52E + 04	3.49E + 03
0.1	0.162	9.04E-03	2.08E-03	6	2.48	1.63E + 04	3.76E + 03
0.11	0.172	3.16E-02	7.28E-03	7	2.74	1.70E + 04	3.91E + 03
0.12	0.182	9.35E-02	2.15E-02	8	3	1.73E + 04	3.98E + 03
0.13	0.192	2.38E-01	5.47E-02	9	3.25	1.74E + 04	4.00E + 03
0.14	0.202	5.31E-01	1.22E-01	10	3.48	1.74E + 04	4.00E + 03
0.15	0.212	1.07E + 00	2.45E-01				

work, becomes significant.

Table 3 shows the numerical values of the total reaction rate depending on the temperature of a star. To orient the correspondence between temperatures and energies, the energy equivalents of temperature (Gamow peak energies) are also presented in the second column.

Conclusions

New experimental data were obtained on the differential cross sections of the reaction $^{11}B(^{10}B,^{9}Be)^{12}C$ at the energy $E_{10_B} = 41.3$ MeV. In this work, we measured the angular distributions for transitions to the ground (0^+) and excited states of the ^{12}C nucleus at energies $E^* = 4.44$ MeV (2^+) and $E^* = 9.64$ MeV (3^-). The analysis of experimental data was carried out on the basis of a modified DWBA (MDWBA) method, assuming a one-step proton transfer mechanism. It is shown that this mechanism dominates at small angles (in the region of the main diffraction maximum of the angular distributions), and the reaction ^{11}B (^{10}B, ^{9}Be)^{12}C at an energy of $^{10}B = 41.3$ MeV is peripheral. This indicates that the (^{10}B,^{9}Be) reaction is a quite suitable tool for finding "indirectly determined" ANC values. Our analysis allowed us to extract the squared ANC values for the $\{^{11}B + p\}$ configurations as 322 ± 76 fm^{-1}, 32.8 ± 8.4 fm^{-1} and 1.26 ± 0.44 fm^{-1} for 0^+, 2^+ and 3^- states of the ^{12}C nucleus, respectively. They are 1.5–2 times larger than the values available in the literature.

The ANC values for low-lying states of the ^{12}C nucleus were used to describe the available experimental data on the S-factors of radiative proton capture with the excitation of these states, and to extrapolate them to the zero-energy region within the framework of a modified R-matrix method. The obtained values of S-factors at zero energy are in excellent agreement with existing literature values, with the exception of the $S(0,\gamma_1)$ value obtained by Kelley et al., which is 3 times lower than our result.

The obtained energy dependence of the astrophysical S-factor was used to determine the $^{11}B(p,\gamma)^{12}C$ reaction rate in the energy region E $\leq$ 3.5 MeV. The reaction rate calculation results show good agreement with NACRE II data. One can also notice a slight deviation at temperatures below $T_9 = 0.1$ K. In our opinion, this discrepancy is caused by the difference in the principles of the theoretical methods used to extrapolate the astrophysical S-factor to the ultra-low energy region in these works.

In this reason, it is required to carry out additional accurate measurements of the experimental values of the cross section (astrophysical S-factor) of the $^{11}B(p,\gamma)^{12}C$ reaction in the energy range E < 100 keV.

CRediT authorship contribution statement

S.K. Sakhiyev: Project administration, Funding acquisition. **S.V. Artemov:** Writing – review & editing, Validation, Methodology, Conceptualization. **N. Burtebayev:** Methodology, Investigation. **S.B. Sakuta:** Methodology, Investigation, Formal analysis. **S.B. Igamov:** Methodology, Investigation, Formal analysis. **Maulen Nassurlla:** Software, Investigation. **K. Rusek:** Validation, Resources, Methodology, Funding acquisition. **M. Wolińska-Cichocka:** Resources, Methodology, Investigation. **N. Amangeldi:** Methodology, Investigation. **Marzhan Nassurlla:** Visualization, Software, Investigation. **A. Trzcińska:** Investigation. **G. Yergaliuly:** Software. **F.Kh. Ergashev:** Writing – original draft, Software, Investigation. **O.R. Tojiboev:** Writing – original draft, Investigation, Formal analysis. **I.Ya. Son:** Investigation, Software. **A. Sabidolda:** Investigation. **R. Khojayev:** Investigation. **Y.B. Mukanov:** Investigation. **D.A. Issayev:** Investigation.

Declaration of competing interest

The authors declare the following financial interests/personal relationships which may be considered as potential competing interests: N. Burtebayev reports financial support was provided by Ministry of Science and Higher Education of the Republic of Kazakhstan. If there are other authors, they declare that they have no known competing financial interests or personal relationships that could have appeared to influence the work reported in this paper.

Acknowledgments

This work is funded by the Ministry of Science and Higher Education of the Republic of Kazakhstan (Grant # AP14870964 “Studies of the interaction of protons and ions ^{10}B with nuclei ^{11}B for thermonuclear and astrophysical applications”).

Data availability

Data will be made available on request.

References

[1] Hoyle F. On nuclear reactions occurring in very hot stars. The synthesis of elements from carbon to nickel. Astrophysical J Suppl Ser Sup 1953;1:121. https://doi.org/10.1086/190005.
[2] Kajino T. Inhomogeneous big-bang model, revived, and evolution of the light elements in cosmic rays. Nucl Phys A 1995;588:339–44. https://doi.org/10.1016/0375-9474(95)00159-x.
[3] Malaney RA, Fowler WA. Late-time neutron diffusion and nucleosynthesis in a post-QCD inhomogeneous Omega(b)=1 universe. Astrophys J 1988;333:14. https://doi.org/10.1093/mnras/237.1.67.
[4] Parpottas Y, et al. The astrophysical S-factor of the 11B(d, n)12C reaction is below 135 keV. Phys Rev C 2006;74:015804. https://doi.org/10.1103/PhysRevC.74.029903.
[5] Kavanaugh LH, Fowler VA, Kavanagh RW, Malaney RA. Signatures of inhomogeneity in the early universe. Astrophys J 1991;372:1. https://doi.org/10.1086/170725.
[6] He JJ. Direct measurement of ^{11}B(p, γ)^{12}C astrophysical S factors at low energies. Phys Rev C 2016;93:055804. https://doi.org/10.1103/PhysRevC.93.055804.
[7] Xu HM, Gagliardi CA, Tribble RE, Mukhamedzhanov AM, Timofeyuk NK. Overall normalization of the astrophysical S factor and the nuclear vertex constant for ^{7}Be (p,γ)^{8}B reactions. Phys Rev Lett 1994;73:2027–30. https://doi.org/10.1103/PhysRevLett.73.2027.
[8] Artemov SV, et al. Asymptotic normalization coefficient for ^{12}C+p→^{13}N from the ^{12}C(^{10}B,^{9}Be)^{13}N reaction and the ^{12}C(p, γ)^{13}N astrophysical S factor. Eur Phys J A 2022;58:24. https://doi.org/10.1140/epja/s10050-021-00652-z.
[9] Artemov SV, Zaparov EA, Nie GK. Asymptotic normalization factors for light nuclei from proton transfer reactions. Bull Russ Acad Sci-Phys 2003;67:1741–6.
[10] Burtebaev N, Igamov SB, Peterson RJ, Yarmukhamedov R, Zazulin DM. New measurements of the astrophysical S factor for ^{12}C(p, γ)^{13}N reaction at low energies and the asymptotic normalization coefficient (nuclear vertex constant) for the ^{13}N→p+^{12}C. Phys Rev C 2008;78:035802. https://doi.org/10.1103/PhysRevC.78.035802.
[11] Artemov SV, Bajajin AG, Igamov SB, Nie GK, Yarmukhamedov R. Nuclear asymptotic normalization coefficients for ^{13}C+p→^{14}N configuration and astrophysical S factor for radiative proton capture. Phys Atom Nucl 2008;71:998–1011. https://doi.org/10.1134/S1063778808060045.
[12] Artemov SV, Igamov SB, Tursunmakhatov QI, Yarmukhamedov R. *Extrapolation of astrophysical S factors for the reaction ^{14}N(p, γ)^{15}O to near-zero energies*. Phys Atom Nucl 2012;75:291–300. https://doi.org/10.1134/S1063778812020032.
[13] Igamov SB, Artemov SV, Yarmukhamedov R, Burtebayev N, Sakuta SB. *Astrophysical S factors for the reaction ^{6}Li(p, γ)^{7}Be at ultralow energies*. J Vestnik Natl Nucl Centre Republic of Kazakhstan 2016;56:82–6.
[14] Nassurlla M, et al. *Scattering of ^{10}B ions on ^{11}B nuclei at an energy of 41.3 Me*V. Eur Phys J A 2024;60:30. https://doi.org/10.1140/epja/s10050-023-01220-3.
[15] Rousseau M, et al. *Highly deformed ^{40}Ca configurations in ^{28}Si+^{12}C*. Phys RevC 2002;66:034612. https://doi.org/10.1103/PhysRevC.66.034612.
[16] Burtebayev N, et al. *Measurement and analysis of ^{10}B+^{12}C elastic scattering at energy of 41.3 MeV*. Int J Mod Phys 2019;E28(4):1950028. https://doi.org/10.1142/S0218301319500289.
[17] Kowalczyk M. *SMAN: A Code for Nuclear Experiments* (Warsaw University report, 1998).
[18] ROOT, *A Data Analysis Framework*, http://root.cern.ch/drupal/.
[19] Gulamov IR, Mukhamedzhanov AM, Nie GK. *Method for selecting peripheral reactions dominated by the pole mechanism: analysis of (d,t) reactions on 1p-shell and ^{19}F nuclei*. Phys At Nucl 1995;58:1689–95.
[20] Artemov SV, Gulamov IR, Zaparov EA, Zotov IY, Nie GK. *The analysis of (^{3}He,d) reactions on 1p-shell nuclei by the method combining DWBA with dispersion approach*. Phys At Nucl 1996;V59.
[21] Mukhamedzhanov AM, Blokhintsev LD. *Asymptotic normalization coefficients in nuclear reactions and nuclear astrophysics*. Eur Phys J 2022;V58. https://doi.org/10.1140/epja/s10050-021-00651-0.
[22] Mukhamedzhanov AM, et al. *Asymptotic normalization coefficients for ^{10}B→^{9}Be+p*. Phys Rev C 1997;56:1302–12. https://doi.org/10.1103/PhysRevC.56.1302.
[23] Tojiboev O, Yarmukhamedov R, Artemov SV, Sakuta SB. *Asymptotic normalization coefficients for ^{7}Be+p→^{8}B from the peripheral ^{7}Be(d,n)^{8}B reaction and their astrophysical application*. Phys Rev C 2016;94:054616. https://doi.org/10.1103/PhysRevC.94.054616.
[24] Yarmukhamedov R, Tursunmakhatov KI, Burtebayev N. *Asymptotic theory of charged particle transfer reactions at low energies and nuclear astrophysics*. Int J Mod Phys Conf Series 2019;49:1960016. https://doi.org/10.1142/S2010194519600164.
[25] Artemov SV, Igamov SB, Tursunmakhatov KI, Yarmukhamedov R. *Determination of nuclear vertex constants (asymptotic normalization coefficients) for the virtual decays ^{3}He→d+p and ^{17}F→^{16}O+p and their use for extrapolating astrophysical S-factors of the radiative proton capture by the deuteron and the ^{16}O nucleus at very low energies*. Bull Russ Acad Sci Phys 2009;V73(N2):165–70. https://doi.org/10.3103/S1062873809020075.
[26] Blokhintsev LD, Borbely I, Dolinskii EI. *Nuclear vertex constants*. Sov J Part Nucl 1977;N8:485.
[27] Ergashev FK, et al. *Asymptotic normalization coefficients for the ^{17}F→^{16}O+p configuration from the ^{16}O(^{10}B,^{9}Be)^{17}F reaction and estimation of the ^{16}O(p,γ)^{17}F astrophysical S-factor*. Acta Physica Polonica B 2022;53:9–15. https://doi.org/10.5506/APhysPolB.53.9-A5.
[28] Nassurlla M, et al. *^{11}B(^{15}N,^{14}C)^{12}C reaction mechanisms and ANC for the ^{15}N→^{14}C+p configuration*. Acta Phys Pol B Proc Suppl 2023;16(2):A14. https://doi.org/10.5506/aphyspolbsupp.16.2-a14.
[29] Nuclear Reaction Video (NRV), *Low Energy Nuclear Knowledge Base*, http://nrv.jinr.ru/nrv/.
[30] Thompson IJ. FRESCO, Department of Physics, University of Surrey, July 2006, GuildfordGU27XH, England, version FRESCO 2.0, http://www.fresco.org.uk/.
[31] XFRESCO: a GUI for Fresco, https://personal.us.es/moro/xfresco/.
[32] Coimbra MM, et al. *Study of the ^{10,11}B+^{10,11}B reactions up to E/A≈5 MeV*. Nucl Phys A 1991;535:161–88. https://doi.org/10.1016/0375-9474(93)90332-r.
[33] Goncharov SA, Dobesh J, Dolinskii EI, Mukhamedzhanov AM, Cejpek J. Sov J Nucl Phys 1982;35:383.
[34] Timofeyuk NK. *Spectroscopic factors and asymptotic normalization coefficients for 0 p-shell nuclei: recent updates*. Phys Rev C 2013;88:044315. https://doi.org/10.1103/PhysRevC.88.044315.
[35] Timofeyuk NK. *Overlap functions, spectroscopic factors, and asymptotic normalization coefficients generated by a shell-model source term*. Phys Rev C 2010;81:064306. https://doi.org/10.1103/PhysRevC.81.064306.
[36] Barker FC, Kajino T. *The ^{12}C(α,γ)^{16}O cross section at low energies*. Aust J Phys 1991;44:369–96. https://doi.org/10.1071/PH910369.
[37] Kelley JH, Purcell JE, Sheu CG. *Energy levels of light nuclei A=12☆*. Nucl Phys A 2017;968:71–253. https://doi.org/10.1016/j.nuclphysa.2017.07.015.
[38] Cecil FE, et al. *Radiative capture of protons by light nuclei at low energies*. Nucl Phys A 1992;539:75–96. https://doi.org/10.1016/0375-9474(92)90236-D.
[39] Kelley JH, et al. *The ^{11}B(p,γ)^{12}C reaction below 100 keV*. Phys Rev C 2000;62:025803. https://doi.org/10.1103/PhysRevC.62.025803.
[40] Huus T, Day RB. *The gamma radiation from ^{11}B bombarded by protons*. Phys Rev 1953;91:599–605. https://doi.org/10.1103/PhysRev.91.599.
[41] Xu Y, Takashi K, Goriely S, Arnould M. *NACRE II:an update of the NACRE compilation of charged-particle-induced thermonuclear reaction rates for nuclei with mass number A<16*Arxiv: 1310.7099v1 [nucl-th] 26 Oct 2013.
[42] Fowler WA, Caughlan GR, Zimmerman BA. *Thermonuclear reaction rates*. Ann Rev Astron Astrophys 1967;5(1):525–70. https://doi.org/10.1146/annurev.aa.05.090167.002521.